Transition-metal Complexes with Nano-sized Phosphine and Pyridine Ligands-Catalysis, Fluxional Behavior and Molecular Recognition

Yasushi Obora, Makoto Tokunaga and Yasushi Tsuji*

Catalysis Research Center and Division of Chemistry, Graduate School of Science, Hokkaido University, CREST, Japan Science and Technology Corporation (JST), Sapporo 001-0021, Japan

Nano-sized phosphine and pyridine ligands having tetraphenylphenyl-, *m*-terphenyl-, poly(benzylether) moieties were synthesized. These ligands showed a remarkable effect in homogeneous transition metal catalyzed reactions. Pd(II) complex with tetraphenylphenyl substituted pyridine ligands show high catalytic activity in oxidation of ketones suppressing Pd black formation and maintains the catalytic activity for a long time. Rh(I) complex catalyst with *m*-terphenyl substituted phosphine ligands showed remarkable rate accerelation toward hydrosilylation of ketones. In addition, several phosphinocalixarene ligands were synthesized and their coordination studies with Pd(II), Pt(II), Ru(II), Ir(I), and Rh(I) metals were documented. Ir(I) and Rh(I) cationic complexes with 1,3,5-triphosphinocalix[6]arene ligand showed dynamic behavior with size-selective molecular recognition.

KEY WORDS: nano-sized ligand; dendrimer; calixarene; phosphine; pyridine; homogeneous catalysis; oxidation; hydrosilylation; ligand effects; molecular recognition

1. Introduction

Since phosphines and pyridines serve as efficient ligands in homogeneous transition-metal catalyzed reactions, design and modification of the ligands have been extensively investigated to realize high catalytic activity and selectivity.[1] However, major trials to modify the ligands have yet been carried out within proximal substitients around the catalyst metal center. For example, very bulky phosphines such as P(*t*-Bu)$_3$ and tricyclohexylphosphine (PCy_3) were utilized to be effective ligands in transition metal catalyzed reactions.[2]

Alternatively, design and preparation of nano-sized ligands with bulky substituents located remotely from catalyst center might be promising, which would show unprecedented catalytic performance. There have been several reports in which nano-sized ligands were used in transition-metal catalyzed reactions, but so far their success was rather limited.[3]

In this review, we summarize recent progress from our laboratoty in the field of nano-sized dendrimer pyridine and phosphine ligands having tetraphenylphenyl-,[4] *m*-terphenyl-,[5] and poly(benzylether) moieties.[6] These ligands show remarkable catalytic performance in Pd-catalyzed alcohol oxidation[4] and Rh-catalyzed ketone hydrosilylation.[5] In addition, we synthesized novel phosphine ligands having calixarene moieties (phosphinocalixarenes).[7-10] Phosphinocalixarenes are attractive ligands since they have well-defined cavity to create a spacially confined nano-sized environment upon complexation with transition metals.[11] Coordination properties of several phosphinocalixarenes with Pd(II), Pt(II), Ru(II) metals[8,9] as well as molecular recognition properties of their Ir(I), and Rh(II) cationic complexes[10] were also documented here.

2. Pd-catalyzed aerobic oxidation of alcohols with pyridine ligands having tetraphenylphenyl moiety[4]

Nano-sized pyridine ligands having tetraphenylphenyl moieties (**1a-e**) were synthesized by utilizing Diels-Alder reaction of ethynylpyridine with corresponding 2,3,4,5-tetraarylcyclopentadienone (Figure 1).[12] Complexation of **1** with $Pd(OAc)_2$ afforded $Pd(OAc)_2(\mathbf{1})_2$ quantitatively. The X-ray structure of $Pd(OAc)_2(\mathbf{1a})_2$ revealed that the 2,3,4,5-tetraphenylphenyl substituent at the 3-position of the pyridine ring spatially spreads out and covers the nano-sized area over the long-range from the Pd center (Figure 2). However, steric congestion around the Pd coordination sphere is essentially the same that of corresponding pyridine complex $Pd(OAc)_2(Py)_2$,[13] implying the large substituent at the 3-position would not obstruct the metal center.

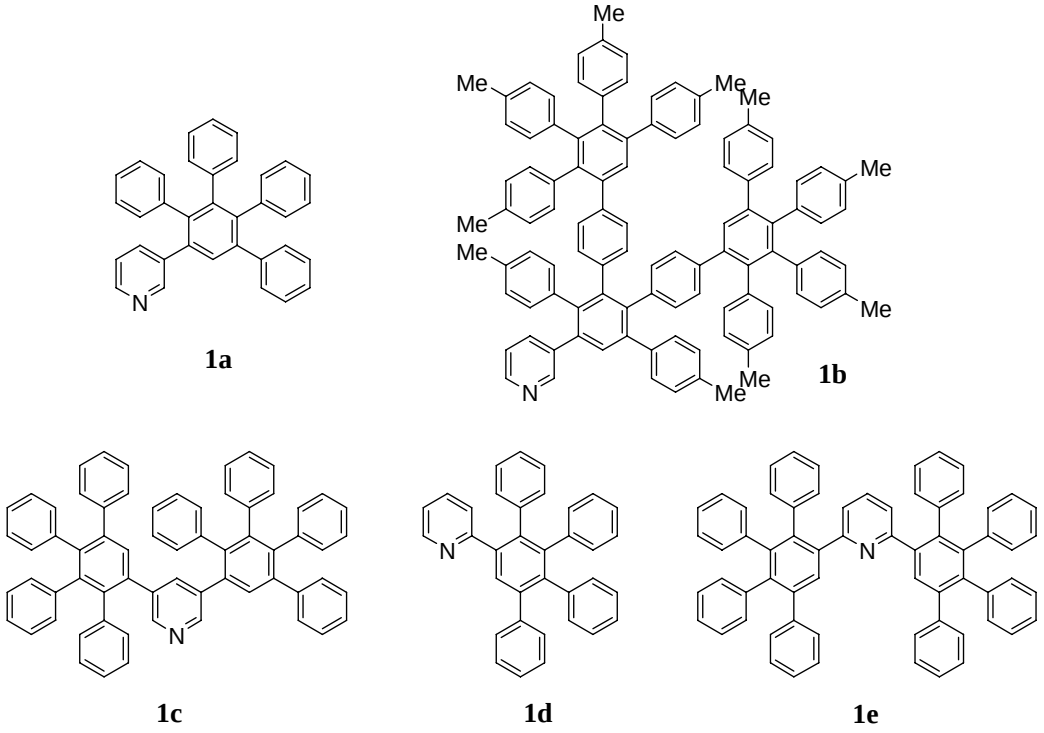

Figure 1. Pyridine ligands having 2,3,4,5-tetraphenylphenyl moiety.

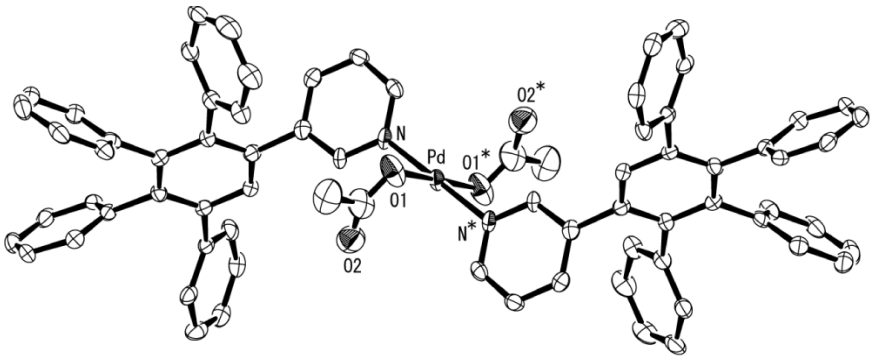

Figure 2. X-ray structure of $Pd(OAc)_2(\mathbf{1a})_2$

To evaluate catalytic performance of the $Pd(OAc)_2(\mathbf{1})_2$ complexes, aerobic oxidation of alcohols was examined (eq 1). Pd catalysts are generally known to show a good catalytic activity in this reaction.[14] However, metal aggregation and precipitation cause catalyst decomposition and a considerable loss of catalytic activity.[14] The presented nano-sized ligands overcome this intrinsic problem of homogeneous Pd catalysts. The result of $Pd(OAc)_2(\mathbf{1})_2$ catalyzed air oxidation of various alcohols are shown in Table 1.

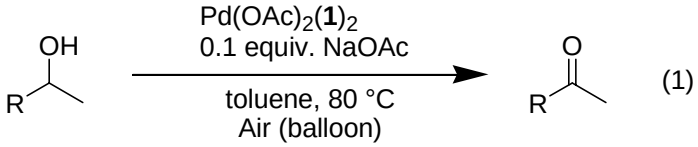

(1)

$Pd(OAc)_2$ and $Pd(OAc)_2(Py)_2$ (Py = pyridine) showed no or low catalytic activity in the oxidation of 1-phenylethanol and the Pd catalyst decomposed completely into Pd black (entries 1-2). Similarly, $Pd(OAc)_2(3\text{-}PhPy)_2$ and $Pd(OAc)_2(3,5\text{-}diPhPy)_2$ resulted in complete Pd black formation within 6 h and yielded acetophenone in ca. 30% (entries 3-4). In contrast, $Pd(OAc)_2(\mathbf{1a})_2$ afforded acetophenone in 87% yield without the Pd black formation (entry 5). The higher dendritic analogue $Pd(OAc)_2(\mathbf{1b})_2$ is more efficient catalyst (entry 6), achieving the highest TON = 1480 with S/C = 2000 (entry 7). $Pd(OAc)_2(\mathbf{1c})_2$ also catalyzed the reaction without the Pd

black formation (entry 8). However, the use of $Pd(OAc)_2$(**1d**)$_2$ and $Pd(OAc)_2$(**1e**)$_2$ as the catalyst resulted in trace yields due to the Pd black formation. The marked effects of **1a** and **1b** over pyridine (Py) ligands were also observed in the oxidation of various alcohols under air (Table 1, entries 9-21). Thus, the spatially spread moiety at the 3-position effectively suppresses the Pd black formation and maintains the catalytic activity for a long time.

Table 1. Effect of pyridine ligands on palladium-catalyzed air oxidation of alcohols[a]

entry	alcohol	ligand[b]	time/h	yield/%[c]	Pd black formation[d]
1	1-phenylethanol	none	24	trace	+
2		Py	24	23	+
3		3-PhPy	6	34	+
4		3,5-diPhPy	6	32	+
5		**1a**	72	87	–
6		**1b**	72	>99 (95)	–
7[e]		**1b**	96	74	–
8		**1c**	72	63	–
9	2-octanol	Py	2	21	+
10		**1a**	96	69	–
11		**1b**	96	79 (75)	–
12	benzyl alcohol	Py	2	23	+
13		**1a**	48	74	–
14		**1b**	48	78	–
15	2-heptanol	Py	8	27	+
16		**1a**	72	52	–
17		**1b**	72	72	–
18	3,3-dimethyl-2-butanol	Py	4	32	+
19		**1a**	96	89	–
20	2-hexanol	Py	2	24	+
21		**1a**	96	72	–

[a] S/C=1000. [b] The ligand of the $Pd(OAc)_2$(ligand)$_2$. [c] Determined by GC. Isolated yields in parentheses. [d] +: Complete Pd black formation. –: No Pd black formation. [e] S/C=2000.

3. Rh-catalyzed hydrosilylation of ketones with the bowl-shaped phosphine as a ligand[5]

The two *m*-terphenyl substituted triarylphosphine ligands, tris(2,2",6,6"-tetramethyl-*m*-terphenyl-5'-yl)phosphine (**2a**)[15] and tri(*m*-terphenyl-5'-yl)phosphine (**2b**) were synthesized by lithiation of the corresponding *m*-terphenyl bromides followed by a reaction with PCl_3.[5]

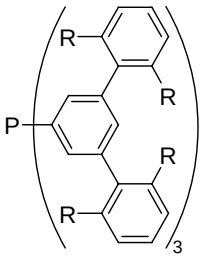

R= Me: **2a**
R= H: **2b**

The ligands **2a** and **2b** were compared with other common phosphine ligands in Rh-catalyzed hydrosilylation of cyclohexanone with $HSiMe_2Ph$ (eq 2, Table 2). In the presence of 0.5 mol% $[RhCl(C_2H_4)_2]_2$ combined with **2a** (P/Rh = 2), the reaction proceeed at room temperature for 3 h and cyclohexanol was obtained in 97% yield after a desilylation (entry 1). In contrast, **2b** afforded the product only in 25% yield under the similar reaction conditions (entry 2). The reactions with other conventional triarylphosphines (entries 3–6) and trialkylphosphines (entries 7–9) were sluggish showing lower catalytic activity than **2a**. Thus the phosphine ligand having methyl substisuents at 2,2",6,6"-positions, **2a**, showed marked rate enhancement effect in the hydrosilylation. A kinetic study indicated that the **2a** ligand realized 154, 31, and 28 times faster reaction than PPh_3, **2b**, and P(*o*-tol)$_3$, respectively.

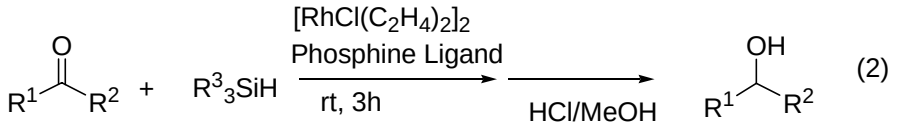

(2)

Table 2. Effects of ligands in the hydrosilylation of cyclohexanone[a]

entry	ligand[b]	yield /%[c]
1	**2a**	97
2	**2b**	25
3	PPh_3	7
4	P(2-furyl)$_3$	22
5	P(*o*-tol)$_3$	32
6	$PMes_3$	25
7	PEt_3	<2
8	PCy_3	<2
9	P(*t*Bu)$_3$	31

[a]Reaction conditions: cyclohexanone (1.0 mmol), $HSiMe_2Ph$ (1.2 mmol), $[RhCl(C_2H_4)_2]_2$ (0.0050 mmol), ligand (0.020 mmol), tridecane (0.25 mmol, as an internal standard), benzene (1.0 mL), rt, 3 h. [b]tol = tolyl, Mes = mesityl, Cy = cyclohexyl. [c]Yield of cyclohexanol by GC after the desilylation with HCl/MeOH.

The rate enhancement with **2a** was also evident using other silanes such as $HSiEt_3$ and ketones such as acetophenone and (–)-menthone (Table 3).

Table 3. Hydrosilylation with various substrates[a]

entry	ketone	silane	ligand	time/h	yield /%[b]
1	cyclohexanone	$HSiEt_3$	**2a**	21	81
2			**2b**	21	36
3			PPh_3	21	13
4	cyclohexanone	$HSiMePh_2$	**2a**	20	97
5			**2b**	20	37
6			PPh_3	20	27
7	acetophenone	$HSiMe_2Ph$	**2a**	5	96
8			**2b**	5	15
9			PPh_3	5	15
10	(–)-menthone	$HSiMe_2Ph$	**2a**	20	92 (45/55)[c]
11			**2b**	20	8 (43/57)[c]
12			PPh_3	20	12 (38/62)[c]

[a]Reaction conditions: ketone (1.0 mmol), silane (1.2 mmol), $[RhCl(C_2H_4)_2]_2$ (0.0050 mmol), ligand (0.020 mmol), tridecane (0.25 mmol, as internal standard), benzene (1.0 mL), rt. [b]Yield of alcohol by GC after the desilylation with HCl/MeOH. [c]Products ratio (neomenthol/menthol).

The bowl-shaped ligand **2a** showed much more high rate enhancement effect than structurally comparable **2b**. The structures of **2a** and **2b** were optimized by HF/6-31G(d)-CONFLEX[16]/MM3[17] calculation and they have nanosized bowl-shaped structures with the phosphorous atom at the bottom (Chart 1). Diameters of the bowl of **2a** and **2b** were 1.99 and 1.95 nm, respectively. The difference in reactivity between **2a** and **2b** cannot simply explain by the steric (cone angle) and electronic effects (basisity) of the phosphine since they have comparable cone angles (205 °for **2a** and 193° for **2b**)[18] and basicities by judging $^{1}J_{P\text{-}Se}$ coupling constants of the phosphine selenides (769.7 Hz for **2a**, 765.5 Hz for **2b**).[19]

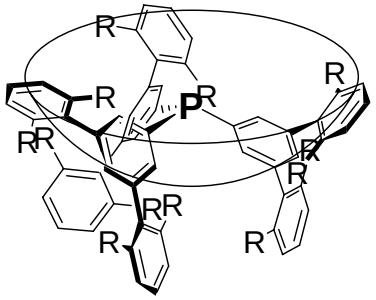

Chart 1

The most important difference between **2a** and **2b** is the depth of the bowl (0.208 nm for **2a** and 0.132 nm for **2a**). This result indicate that the deeper bowl-shaped **2a** ensures substantial empty space around the phosphorus atom and, at the same time, is bulky enough to provide a low coordinated species with a rhodium metal. This long-range steric effect of **2a** prevailed the formation of Rh mono-phosphine spiecies which facilitate the rate enhancement toward hydrosilylation.

4. Nano-sized Pt(0)-phosphine complexes having polybenzylether moiety[6]

Mono- (**3a-c**) and bidentate (**3d-e**) dendrimer-phosphine ligands connecting

Frećhet type poly(benzylether) unit were synthesized as shown in Figure 2. The defect-free monodisperse nature of **3** was confirmed by ^{31}P NMR and ESI mass spectra.

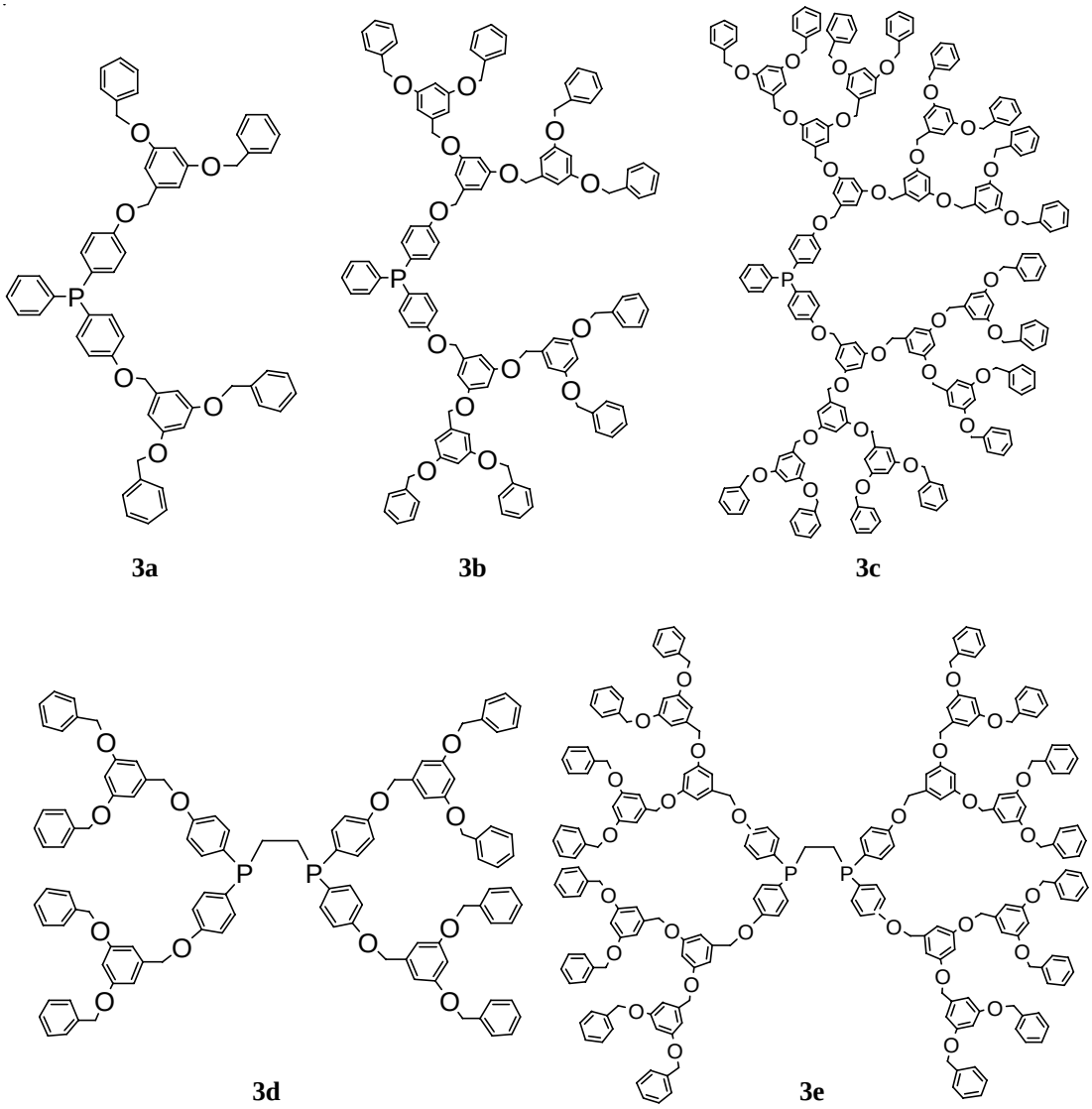

Figure 2. Monodentate and bidentate phosphine ligands of monodentate with poly(benzylether) dendrimer units.

Two equiv of **3a** and **3b** was allowed to react with $PtCl_2$(COD) at room temperature gave *cis*-$PtCl_2$(**3a**)$_2$ and *cis*-$PtCl_2$(**3b**)$_2$ complexes in high yields (Scheme 1).

Subsequently, reduction of *cis*-$PtCl_2$(**3a**)$_2$ and *cis*-$PtCl_2$(**3b**)$_2$ with $NaBH_4$ gave corresponding Pt(0) complexes (Scheme 1). The presented metal complexes posses one metal at core and the metal is surrounded by nanosized dendrimer moiety. The ^{31}P NMR of the Pt(0) complexes shows the signals at 48.2-49.0 ppm with $^1J_{P\text{-}Pt}$ coupling of 4445-4455 Hz. These chemical shifts as well as the $^1J_{P\text{-}Pt}$ values are very similar with those of $Pt(PPh_3)_3$ (49.9 ppm, $^1J_{P\text{-}Pt}$ = 4438 Hz),[20] but not with $Pt(PPh_3)_4$ (9.2 ppm, $^1J_{P\text{-}Pt}$ = 3829 Hz).[20] Thus the ligands (**3a** and **3b**) gave tris complex Pt(**3**)$_3$. The use of excess of ligand did not yield the tetrakis complex. This may be attributed to the voluminous size of the dendrimer phosphine ligands.[21] With the chelating phosphines (**3d** and **3e**), bis-Pt(0) complexes (Pt(**3d**)$_2$ and Pd(**3e**)$_2$) were obtained in high yields by the reaction of $PtCl_2$(COD) followed by reduction with $NaBH_4$.

Scheme 1. Synthesis of Pt(II) and Pt(0) complexes with monodentate dendrimer-phosphine ligands (**3a,b**)

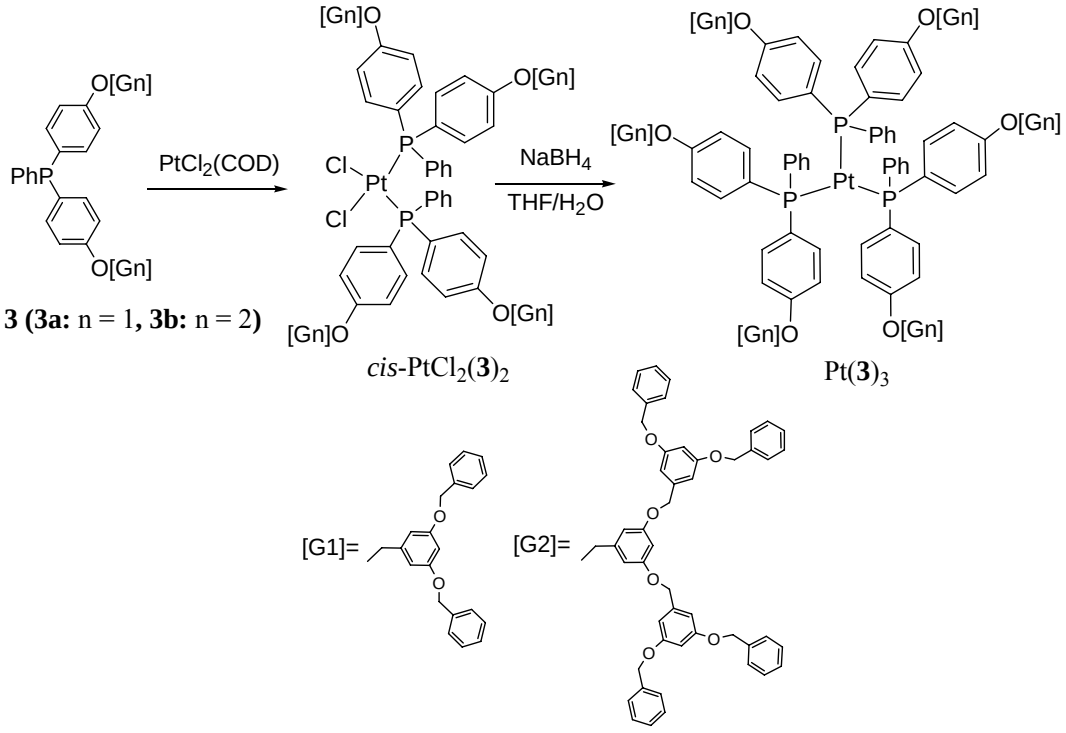

3 (3a: n = 1**, 3b:** n = 2**)**

cis-$PtCl_2$(**3**)$_2$

Pt(**3**)$_3$

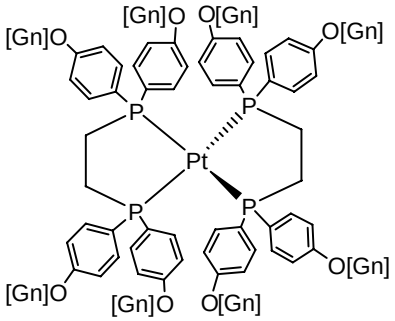

Pt(**3d**)$_2$: n = 1, Pt(**3e**)$_2$: n = 2

Figure 3. Pt(0) complexes of bidentate dendrimer-phosphine ligands (**3d** and **3e**)

The molecular modeling of **3e** showed the Pt(0) complex has nanosized flattened globular structure and the diameter of **3e** is estimated to be 4.4 nm. Furthermore, several cavities appeared around the Pt, which might be utilized as a guest room in some catalytic transformations.

5. Nano-sized metal-phosphine complexes having calix[4]arene moiety

5-1. Preparation and complexation of tetraphosphinocalix[4]arene adopting partial cone[7] and 1,3-alternate conformations[8]

We synthesized two kinds of tetraphosphinocalix[4]arenes (**4a** and **4b**) ligands adopting partial cone (**4a**) and 1,3-alternate (**4b**) conformations (Figure 4).

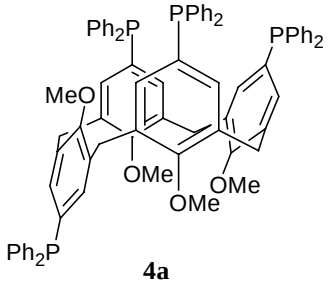

4a

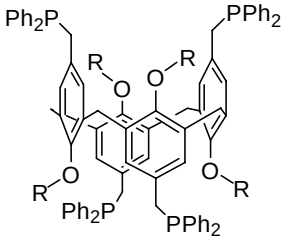

R = *n*-Pr (**4b**)

Figure 4. Tetraphinocalix[4]arene ligand (**4**) adopting partial cone and 1,3-alternate conformations

4a was prepared by lithiation of the corresponding tetrabromocalix[4]arene with *n*-BuLi, followed by phosphination with chlorodiphenylphosphine.[7] X-ray crystallographic analysis and CPMAS solid-state NMR measurements of **4a** elucidated that **4a** adopts a partial cone conformation. The ^{1}H and ^{13}C NMR spectra measured in CD_2Cl_2 at –20 °C results are supported the partial cone structure of **4a** in solution, as observed in the solid state. For example, ^{13}C NMR spectrum exhibit three resonances of the methoxy carbons at 61.8, 62.7, and 63.6 ppm in a 1:1:2 ratio and the two resonances of the methylene carbons at 31.5 ppm and 37.3 ppm in a 1:1 ratio.[22] However, a variable-temperature ^{31}P NMR measurement shows a fluxional behavior of **4a** on NMR time scale due to annulus rotation. Ab initio molecular calculation (HF/6-31G*//HF/STO-3G) showed that the partial cone conformation is the most stable form, while the cone and the 1,3-alternate conformers are only slightly less stable by 2.7 kcal/mol and 4.5 kcal/mol, respectively.

Another tetraphosphinocalix[4]arene **4b** was synthesized *via* Arbuzov phosphinylation of tetra(chloromethyl)calix[4]arene with Ph_2POEt, tetra-*O*-propylation with n-PrI/K_2CO_3, followed by reduction with $PhSiHCl_2$.[8] The ^{1}H and $^{13}C\{^{1}H\}$ NMR spectra of **4b** showed singlet proton resonance at 3.24 ppm and a singlet carbon resonance at 36.0 ppm assignable to the bridging methylene group. These results were in full agreement with a 1,3-alternate conformation of **4b**.[22] Complexation of **4b** with Ru(II) was carried out. The reaction of **4b** with 2 equiv of $[RuCl_2(p\text{-cymene})]_2$ in CH_2Cl_2 afforded the tetranuclear ruthenium complex $[\{RuCl_2(p\text{-cymene})\}_4 \cdot \mathbf{4b}]$ as 1,3-alternate conformer (eq 3).

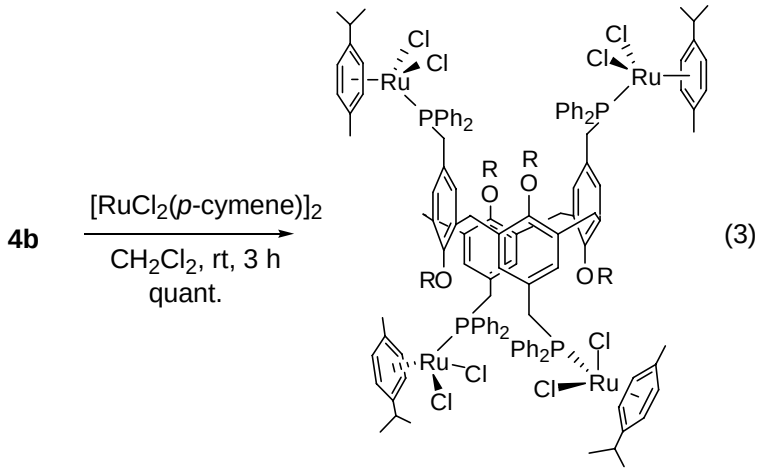

5-2. Fluxional behavior of nano-sized Pt(II) and Pd(II) complexes of bis(diphenylphosphino)calix[4]arene (5)[9]

The diphosphinated calix[4]arene **5** was prepared by lithiation with *n*-BuLi of corresponding dibromocalix[4]arene, followed by phosphination with chlorodiphenylphosphine.[9] In the ^{1}H and $^{13}C\{^{1}H\}$ NMR spectra of **5**, bridging methylene proton resonance appeared as two doublets with a geminal coupling (14 Hz) at 2.90 and 4.22 ppm and the bridging methylene carbon resonance afforded a singlet at 31.3 ppm. These data are all indicative of a cone conformation of **5** in solution-state.[22] Variable-temperature ^{1}H NMR spectra of **5** in a range of –50 to +70 °C showed no significant change and indicated the cone conformation is stable.

5

Reaction of **5** with $PdCl_2$(cod) under dilute condition results in formation of the *trans* coordinated *dinuclear* complex $[PdCl_2(\mathbf{5})]_2$ (Scheme 2 (i)). X-ray structure of $[PdCl_2(\mathbf{5})]_2$ reveals that the two phosphinocalix[4]arene molecules are linked by the two

$PdCl_2$ fragments (Figure 5). The compound $[PdCl_2(\mathbf{5})]_2$ is nano-sized molecule and the distance of the two Pd atoms are 13.187(2) Å. On the other hand, reaction of **5** with $PtCl_2$(cod) affords the *cis* chelating *mononuclear* complex $PtCl_2(\mathbf{5})$ (Scheme 2 (ii)). The CPMAS solid state and solution $^{31}P\{^1H\}$NMR spectrum measured at –80 °C showed two inequivalent phosphine resonances in equal intensities. The $^{13}C\{^1H\}$ NMR spectrum of measured at –80 °C in CD_2Cl_2 showed *four* inequivalent bridging methylene carbons with the same intensity. These observations clearly indicate $PtCl_2(\mathbf{5})$ has C_1 symmetry in solution at –80 °C and in solid state. In addition, **5** reacted with $[Pd(\eta^3\text{-}C_3H_5)(cod)]BF_4$ to afford *mononuclear* cationic complex $[Pd(\eta^3\text{-}C_3H_5)(\mathbf{5})]BF_4$ (Scheme 2 (iii)). The low-temperature $^{31}P\{^1H\}$ and $^{13}C\{^1H\}$NMR measurements suggest that $[Pd(\eta^3\text{-}C_3H_5)(\mathbf{5})]BF_4$ exists as 5: 2 mixture of two stereoisomers possessing a C_1 symmetry.

Scheme 2.

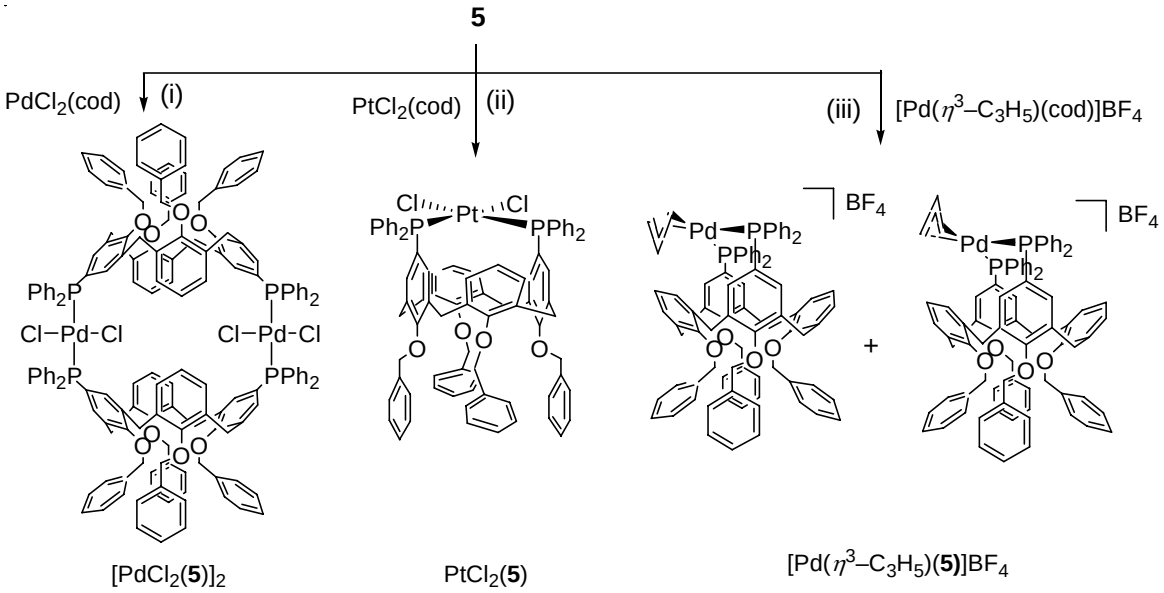

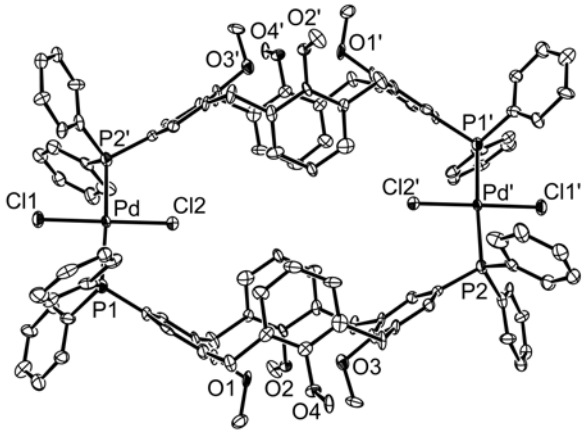

Figure 5. X-ray structure of $[PdCl_2(\mathbf{5})]_2$. Phenyl rings of the benzyl moieties are omitted for clarity.

Although $PtCl_2(\mathbf{5})$ exhibit C_1 structure in solution at –80 °C, variable-temperature NMR spectra show the fluxional behavior. At 20 °C, the $^{31}P\{^1H\}$ NMR spectrum changed into one sharp *singlet* with ^{195}Pt satellites and the $^{13}C\{^1H\}$ NMR spectrum showed a *singlet* peak for the bridging methylene carbons. This observation clearly indicate the symmetry of $PtCl_2(\mathbf{5})$ changes from C_1 to C_{2v} by raising the temperature. Similar fluxional behavior in solution state was observed in $[Pd(\eta^3\text{-}C_3H_5)(\mathbf{5})]BF_4$ and the C_1 symmetry of the compound at –80 °C is changed to C_S symmetry at 20 °C. The behaviors are caused by two separable motions: roll-over motion of the coordination plane (R-motion) and twist motion of the calix[4]arene scaffold (T-motion)[9] (see Scheme 3 for R-motion of $PtCl_2(\mathbf{5})$). Activation enthalpy ($\Delta H^{\ddagger}$ = 41 ± 0.9 kJ mol^{-1}) for the whole fluxional process of $PtCl_2(\mathbf{5})$ were determined by simulating[23] of variable-temperarure ^{31}P NMR. Furthermore, similar simulation[23] afforded activation enthalpies of R motion ($\Delta H^{\ddagger}$ = 41 ± 1.4 kJ mol^{-1}) and T-motion ($\Delta H^{\ddagger}$ = 43 ± 1.5 kJ mol^{-1}) for $[Pd(\eta^3\text{-}C_3H_5)(\mathbf{5})]BF_4$ complex.

Scheme 3

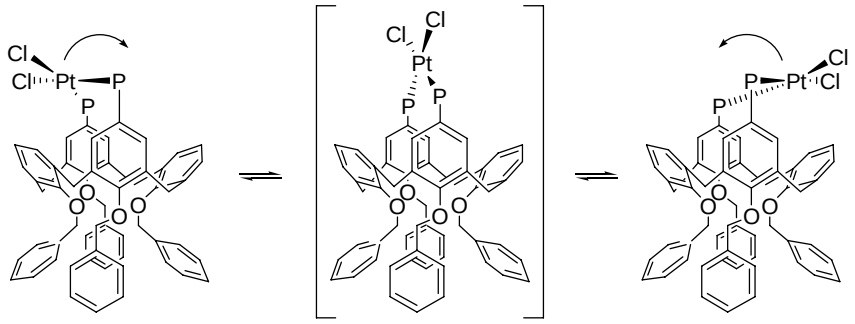

6. Dynamic motion with size-selective molecular encapsulation with nano-sized Ir(I) and Rh(I) cationic complexes with triphosphinocalix[6]arenes[10]

With regard to the phosphinocalixarene ligand having a bigger cavity, a calix[6]arene having three diphenylphosphinomethyl moieties (**6**) was synthesized. ^{1}H, $^{13}C\{^{1}H\}$NMR, and X-ray crystallographic analysis showed **6** has a cone conformation.[10]

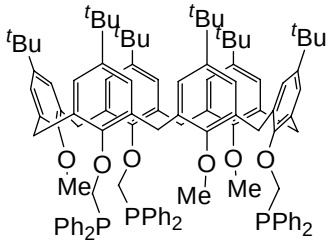

6

The triphosphinocalix[6]arene ligand **6** react with $[Ir(COD)_2]X$ (X = BF_4 and BPh_4 and $[Rh(COD)_2]BF_4$ at room temperature in CH_2Cl_2 for 3 h to afford nano-sized Ir(I) (**7a** and **7b**) and Rh (I) cationic complex (**7c**) in high yields (eq 4).

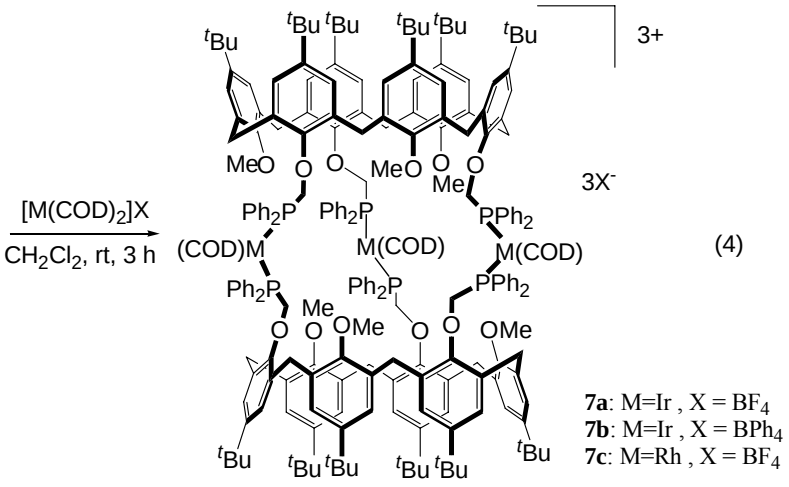

7a: M=Ir , X = BF_4
7b: M=Ir , X = BPh_4
7c: M=Rh , X = BF_4

(4)

X-ray crystal analysis showed **7a** has a capsule-shaped structure having three iridium metals and two calix[6]arene moieties (Figure 6). The complex possessed an inner nano–sized cavity and one CH_2Cl_2 molecule was encapsulated in the cavity. In the structure of **7a**, three inequivalent phosphorous atoms (P1, P2, and P3) existed in a 1: 1: 1 ratio. In solution, the $^{31}P\{^1H\}$ NMR spectrum of **7a** in CD_2Cl_2 at 25 °C showed one broad peak at 16.3 ppm, whereas the NMR spectrum in $Cl_2CDCDCl_2$ at 25 °C showed three ^{31}P resonances at 15.3 (d, ^2J(P,P) = 18 Hz), 15.9 (d, ^2J(P,P) = 18 Hz), and 16.4 (s) ppm (Figure 7). Activation enthalpies for these dynamic behaviors which equalized the three P atoms were determined by simulating[23] these spectra at various temperatures: $\Delta H^{\ddagger}$ = 27 (1) kJ mol^{-1} in CD_2Cl_2 and 64(3) kJ mol^{-1} in $Cl_2CDCDCl_2$. The above-mentioned results indicated that the dynamic motion of **7a** was dependent on the solvent size. The Rh(I) analogue **7c** showed the similar solvent-dependent $^{31}P\{^1H\}$ NMR spectra.

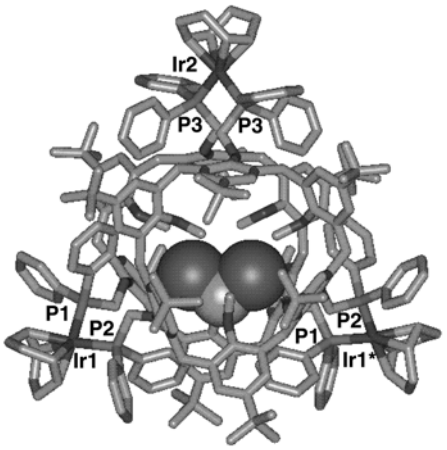

Figure 6. X-ray structure of cationic part of **7a**

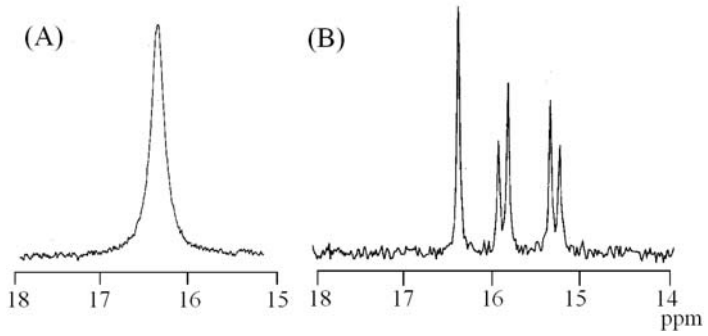

Figure 7. $^{31}P\{^{1}H\}$ NMR spectra of **7a** in (A) CD_2Cl_2 and (B) $Cl_2CDCDCl_2$

The above mentioned phenomenon may be caused by size sensitivity inherent in the cavity of **7a** and **7c**. Thus the $^{31}P\{^{1}H\}$ NMR spectra of **7a** were measured in the presence of various organic molecules to investigate the sensitivity of the cavity (Table 4). As a result, these molecules in Table 4 can be classified into three groups: group A (V < 81 Å^3 and A < 45 Å^2, entries 1-4), group B (V = 81 – 105 Å^3 and A = 45 – 68 Å^2, entries 5-9), and group C (V > 105 Å^3 and A > 68 Å^2, entries 10-13) estimated by using Connolly solvent-excluded volume (V)[24] and maximum projection area (A)[10] of the solvent accessible surface of structures[25] on the B3LYP/6-31G(d,p) optimized structure. Molecules in the group A showed one broad ^{31}P resonances having a significant variations of $\Delta\nu$ values (197–315 Hz). The group B showed three different ^{31}P resonances, indicating the dynamic behaviors were sufficiently slow on the NMR time scale at 25 °C. The molecules in group C showed one broad ^{31}P resonances, but with comparable $\Delta\nu$ values (212－218 Hz). Thus the molecules in group A may be too small to fit the cavity of **7a**, the molecules in group B are just-fitted in the cavity, and the molecules in group C are too large to enter the cavity. It is of particular interest that present Ir(I) and Rh(I) phosphine complexes (**7a** and **7c)** have such a dynamic motion with size-selective molecular encapsulation in organic solvents.

Table 4. $^{31}P\{^{1}H\}$NMR of **7a** with various molecules[a]

	entry	molecule ^{31}P resonances /ppm	V^b/ Å^3	A^c/Å^2
A	1	CH_2Cl_2, 16.9 ($\Delta\nu$ = 197 Hz)	52.9	35.9
	2	$ClCH_2CH_2Cl$, 17.1 ($\Delta\nu$ = 238 Hz)	70.2	40.9
	3	$CHCl_3$, 17.3 ($\Delta\nu$ = 210 Hz)	67.7	42.0
	4	CCl_4, 17.0 ($\Delta\nu$ = 315 Hz)	80.5	42.2
B	5	$Cl_2CHCHCl_2$ 16.7 (d, *J* = 17 Hz), 17.2 (d), 17.8 (s)	100.3	49.5
	6	2,3-dimethyl-2-butene 16.7 (d, *J* = 17 Hz), 17.2 (s), 17.3 (d)	92.0	57.0
	7	toluene 17.2 (d, *J* = 17 Hz), 18.0 (s), 18.1 (d)	87.6	62.1
	8	*o*-xylene 17.5 (d, *J* = 18 Hz), 18.1 (s), 18.2 (d)	103.9	66.7
	9	*m*-xylene 17.4 (d, *J* = 18 Hz), 18.1 (s), 18.2 (d)	104.2	67.2
C	10	cumene, 17.7 ($\Delta\nu$ = 216 Hz)	123.1	68.1
	11	*p*-xylene, 17.8 ($\Delta\nu$ = 212 Hz)	105.6	69.0
	12	mesitylene, 17.2 ($\Delta\nu$ = 218 Hz)	122.0	78.1
	13	5-*t*-butyl-*m*-xylene, 17.4 ($\Delta\nu$ = 214 Hz)	176.3	83.1

[a]**7a** (5 mM) in the presence of the molecule (30% v/v) in $CDCl_3$ at 25 °C.
[b]Connolly solvent-excluded volume. [c]Maximum projection area of the solvent accessible surface.

7. Conclusion

A variety of nano-sized ligand having having tetraphenylphenyl-, *m*-terphenyl-, poly(benzylether), and calix[n]arene (n = 4 and 6) unit have been synthesized. The transition-metal complexes with the present ligands showed remarkable effects in homogeneous catalysis, unique fluxional behavior in solution, and molecular recognition properties during dynamic motion.

References

[1] (a) L. Brandsma, S. F. Vasilevsky and H. D. Verkruijsse, Applications of Transition Metal Catalysts in Organic Synthesis, Springer, Berlin, 1999; (b) Homogeneous Catalysis with Metal Phosphine Complexes (Ed.: L. H. Pignolet), Plenum, New York, 1983. (c) J. P. Collman, L. S. Hegedus, J. R. Norton and R. G. Finke, Principles and Applications of Organotransition Metal Chemistry, University Science Books, Mill Valley, CA, 1987.

[2] (a) A. F. Littke, C. Dai and G. C. Fu, J. Am. Chem. Soc. 122 (2000) 4020; (b) J. H. Kirchhoff, C. Dai and G. C. Fu, Angew. Chem., Int. Ed. 41 (2002) 1945; (c) A. F. Littke and G. C. Fu, Angew. Chem., Int. Ed. 41 (2002) 4176; (d) N. Kataoka, Q. Shelby, J. P. Stambuli and J. F. Hartwig, J. Org. Chem. 67 (2002) 5553; (e) S. D. Walker, T. E. Barder, J. R. Martinelli and S. L. Buchwald, Angew. Chem., Int. Ed. 43 (2004) 1871.

[3] (a) A.-M. Caminade, V. Maraval, R. Laurent and J.-P. Majoral, Curr. Org. Chem. 6 (2002) 739; (b) D. de Groot, B. F. M. de Waal, J. N. H. Reek, A. P. H. J. Schenning, P. C. J. Kamer, E. W. Meijer and P. W. N. M. van Leeuwen, J. Am. Chem. Soc. 123 (2001) 8453; (c) T. Mizugaki, M. Murata, M. Ooe, K. Ebitani and K. Kaneda, Chem. Commun. (2002) 52; (d) V. Maraval, R. Laurent, A.-M. Caminade and J.-P. Majoral, Organometallics, 19 (2000) 4025; (e) Q.-H. Fan, Y.-M. Chen, X.-M. Chen, D.-Z. Jiang, F. Xi and A. S. C. Chan, Chem. Commun. (2000) 789; (f) V. F. Slagt, J. N. H. Reek, P. C. J. Kamer and P. W. N. M. van Leeuwen, Angew. Chem. Int. Ed., 40 (2001) 4271.

[4] T. Iwasawa, M. Tokunaga, Y. Obora and Y. Tsuji, J. Am. Chem. Soc., 126 (2004) 6554.

[5] O. Niyomura, M. Tokunaga, Y. Obora, T. Iwasawa and Y. Tsuji, Angew. Chem. Int. Ed, 42 (2003) 1287.

[6] B. S. Balaji, Y. Obora, D. Ohara, S. Koide and Y. Tsuji, Organometallics, 20 (2001) 5342.

[7] K. Takenaka, Y. Obora, L. H. Jiang and Y. Tsuji, Bull. Chem. Soc. Jpn. 74 (2001) 1709.

[8] K. Takenaka, Y. Obora, L. H. Jiang, and Y. Tsuji, Organometallics, 21 (2002) 1158.

[9] K. Takenaka, Y. Obora and Y. Tsuji, Inorg. Chim. Acta, 357 (2004) 3895.

[10] Y. Obora, Y. Liu, L. Jiang, K. Takenaka, M. Tokunaga and Y. Tsuji, Organometallics, 24 (2005) 4.

[11] (a) C. Wiser, C. B. Dielman and D. Matt., Coord. Chem. Rev., 165 (1997) 93; (b) I. Neda, T. Kaukorat and R. Schmutzler, Main Group Chem. News 6 (1998) 4.

[12] S. Setayesh, A. C. Grimsdale, T. Weil, V. Enkelmann, K. Müllen, F. Meghdadi, E. J. W. List and G. Leising, J. Am. Chem. Soc., 123 (2001) 946.

[13] S. V. Kravtsova, I. P. Romm, A. I. Stash and V. K. Belsky, Acta Crystallogr., Sect. C, 52 (1996) 2201.

[14] (a) T. Nishimura, T. Onoue, K. Ohe and S. Uemura, J. Org. Chem. 64 (1999) 6750. (b) B. A. Steinhoff and S. S. Stahl, Org. Lett. 4 (2002) 4179; (c) M. J. Schultz, C. C. Park and M. S. Sigman, Chem. Commun**.** 24 (2002) 3034; (d) G.-J. ten-Brink, I. W. C. E. Arends and R. A. Sheldon, Science 287 (2000) 1636. (e) G.-J. ten-Brink, I. W. C. E. Arends, M. Hoogenraad, G. Verspui and R. A. Sheldon, Adv. Synth. Catal. 345 (2003) 1341. (f) D. R. Jensen, M. J. Schultz, J. A. Mueller and M. S. Sigman, Angew. Chem., Int. Ed. 42 (2003) 3810. (g) N. Kakiuchi, Y. Maeda, T. Nishimura and S. Uemura, J. Org. Chem. 66 (2001) 6620; (h) R. C. Larock and K. P. Peterson, J. Org. Chem. 63 (1998) 3185; (i) K. Hallman and C. Moberg, Adv. Synth. Catal., 343 (2001) 260.

[15] (a) K. Goto, Y. Ohzu, H. Sato and T. Kawashima, Abstr. Pap. 15th Int. Conf. Of

Phosphorous Chemistry (Sendai, Japan) 2001, p. 236; (b) K. Goto, Y. Ohzu, H. Sato and T. Kawashima, Phosphorus, Sulfur and Silicon 177 (2002) 2179.

[16] (a) H. Goto, J. Am. Chem. Soc. 111 (1989) 8950; (b) H. Goto and E. Osawa, J. Chem. Soc. Perkin Trans. 2 (1993) 187;

[17] (a) J.-H. Lii and N. L. Allinger, J. Am. Chem. Soc. 111 (1989) 8566; (b) J.-H. Lii and N. L. Allinger, J. Am. Chem. Soc. 111 (1989) 8576.

[18] (a) In the present study, we determined the cone angles[18b] using structures optimized by CONFLEX/MM3 and HF/6-31G(d); (b) C. A. Tolman, Chem. Rev. 77 (1977) 313.

[19] D. W. Allen, B. F. Taylor, J. Chem. Soc. Dalton Trans. (1982) 51.

[20] A. Sen, J. Halpern, Inorg. Chem., 19 (1980) 1073.

[21] D. J. Darensbourg, T. J. Decuir, N. W. Stafford, J. B. Robertson, J. D. Draper, J. H. Reibenspies, A. Kathó, F. Joó, Inorg. Chem., 36 (1997) 4218. (b) S. Otsuka, T. Yoshida, M. Matsumoto, K. Nakatsu, J. Am. Chem. Soc., 98 (1976) 5850. (c) C. A. Tolman, W. C. Seidel, D. H. Gerlach, J. Am. Chem. Soc., 94 (1972) 2669.

[22] (a) K. Iwamoto, A. Ikeda, K. Araki, T. Harada, S. Shinkai, Tetrahedron 49 (1993) 9937; (b) J. O. Magrans, J. de Mendoza, M. Pons, P. Prados, J. Org. Chem. 62 (1997) 4518; (c) C. Jaime, J. de Mendoza, P. Prados, P. M. Nieto, C. Sánchez, J. Org. Chem. 56 (1991) 3372.

[23] gNMR version 4.1; Cherwell Scientific Limited.

[24] M. L. Connoly, J. Am. Chem. Soc., 197 (1985) 1118.

[25] M, L. Connoly, Science, 221 (1983) 709.